JMEPEG (1995) 4: 563-572 ©ASM International

Effect of Binder-Phase Modification and Cr_3C_2 Addition on Properties of WC-10Co Cemented Carbide

D. Banerjee, G.K. Lal, and G.S. Upadhyaya

For production of fine-grained and corrosion-resistant tungsten carbide (WC) based cemented carbides, addition of chromium carbide (Cr_3C_2) in small amounts is standard practice. No systematic study, however, has been made of the effects of large additions (maximum 6 wt%) of Cr_3C_2 as a substitute for tungsten carbide. This study focuses on the effect of hard-phase substitution by Cr_3C_2 in WC-10Co cemented carbide. An attempt is also made to modify the binder metal cobalt by partial or complete substitution of nickel. Specimens were prepared using the standard liquid-phase sintering process and were tested for sintered porosity, mechanical properties, corrosion resistance, and microstructural parameters. Results confirm the findings of earlier workers regarding grain refinement and improvement of mechanical properties upon the addition of small amounts (<2 wt%) of Cr_3C_2. Modification of the binder phase improves indentation fracture toughness and corrosion resistance. Addition of Cr_3C_2 independent of the binder type improves corrosion resistance.

Keywords

binder-phase/hard-phase modification in hard metals, corrosion resistance of cemented carbides, hard metal, liquid-phase sintering, mechanical properties of cemented carbides, WC-10Co cemented carbides

1. Introduction

THE exceptional wear/abrasion resistance, high hardness, good fracture toughness, and good compressive strength of tungsten carbide/cobalt (WC-Co) hard metals have led to their extensive use for cutting tools, metalforming tools, mining tools, and wear-resistant parts. Chromium carbide (Cr_3C_2) has been used in small amounts in WC-Co cemented carbides as a grain growth inhibitor. At the same time, Cr_3C_2 has been found to affect other properties (Ref 1-9). Nickel, which is less expensive and more readily available than cobalt, has been tried as a possible substitute for cobalt binder either alone or in combination with iron (Ref 1, 10-16). However, simultaneous substitution of WC and cobalt by Cr_3C_2 and nickel, respectively, has not been tried in a systematic manner. In the present work on WC-10Co cemented carbides, Cr_3C_2 is substituted for WC and the binder cobalt is modified by nickel. The effects of these substitutions on various properties are reported.

2. Experimental Procedure

2.1 *Raw Materials and Their Characterization*

The characteristics of the raw materials used in the present study can be summarized as:

Tungsten carbide powder	
Source	WIDIA Ltd., India
Average particle size, μm	3.2
Total carbon, %	6.12
Free carbon, %	0.10
Chromium carbide powder	
Source	Morton Thiokol Inc., USA
Purity, %	99.5
Particle size	0.3 wt% above 17 μm
	50 wt% above 7 μm
	90 wt% above 2 μm
	100 wt% above 1.5 μm
Ultrafine cobalt powder	
Source	Sherritt Gordon Ltd., Canada
Chemical analysis (typical), %	
Nickel	0.2
Silver	0.3
Iron	0.005
Copper	0.001
Carbon	0.18
Sulfur	0.008
Oxygen	0.7
Fisher subsieve size (FSSS)	0.8
Apparent density, g/cm^3	1.3
Tap density, g/cm^3	2.5
Surface area, m^2/g	2.0-3.0
Particle shape	Spherical loose agglomerates
Oxygen per unit area, g/m^2	2.3×10^{-3} to 3.5×10^{-3}
Nickel powder	
Source	INCO, U.K. (type 123)
Average particle size, μm	3.7
Chemical analysis (typical), %	
Carbon	0.06
Iron	0.005
Oxygen	0.05
Calcium	0.0003
Nitrogen	0.003
Sulfur	0.003
Other	0.001

2.2 *Specimen Preparation*

The premixes of carbides and binder metals were prepared by conventional ball milling. Wet milling of the powders in ace-

D. Banerjee, G.K. Lal, and **G.S. Upadhyaya,** Indian Institute of Technology, Kanpur 208016, India

tone was performed for 36 h in a centrifugal-type ball mill. The additive hard phase (i.e., Cr_3C_2) was initially milled with the binder powder for 8 h, followed by WC addition and an additional 28 h of wet milling. Four hours before the completion of milling, 2 wt% micronized wax powder was added to the charge to improve green strength.

The starting composition of the cemented carbide (WC-10Co) corresponded to approximately 16.5 vol% binder phase. All subsequent compositions were tailored so that the volume fractions of hard phase and binder remained in the same proportions as those of the initial WC-10Co cemented carbide (Table 1).

Rectangular green compacts approximately 25 by 8 by 5 mm^3 in size were pressed from the ball-milled powder premix. A green density of 55 to 60% of theoretical was obtained for all compositions.

The green compacts were dewaxed in a tubular furnace at 400 °C for 2 h in a dry hydrogen atmosphere (–35 °C dew point). The heating rate was maintained at a relatively low value of about 2 °C/min to ensure that the green compacts did not distort during dewaxing.

The dewaxed compacts were subsequently sintered in hydrogen in the same tubular furnace for 1 h at 1420 °C for the grade containing cobalt and at 1470 °C for the other grades containing cobalt/nickel and nickel as binders. The heating rate was approximately 8 °C/min during this stage.

2.3 *Testing and Evaluation*

2.3.1 Sintered Density

The sintered density was measured according to the following formula by using the displacement method (Ref 17):

$$\text{Sintered density } (g/cm^3) = \frac{a}{b - c}$$

where a is the weight of the compact in air, b is the weight of the xylene-impregnated compact in air, and c is the weight of the xylene-impregnated compact in water (all in grams). The theoretical density of each composition was calculated from the simple rule of mixture, taking the theoretical density of various elements and compounds from the literature (WC = 15.77 g/cm^3, Cr_3C_2 = 6.74 g/cm^3, Co = 8.85 g/cm^3, and Ni = 8.90 g/cm^3).

2.3.2 Microstructural Studies

Selected sintered compacts were wet polished primarily on a cast iron wheel using 7 μm diamond paste, followed by finer polishing with diamond pastes of decreasing grit size (4.5 and 2.5 μm). The polished specimens were electroetched using 5% HCl solution at a potential difference of 3 V for 20 to 30 s. They were then placed under a scanning electron microscope (SEM) in secondary electron mode at an operating voltage of 20 kV. About four photomicrographs of each sample were taken arbitrarily from different specimen locations (magnification, 5000×) for subsequent quantitative metallographic study.

Different microstructural parameters—mean linear intercept grain size, contiguity, and binder mean free path—were measured in accordance with the method suggested by Gurland (Ref 18) using the following formulas:

- Carbide mean linear intercept grain size

$$\bar{L}_\alpha = \frac{2(V_V)_\alpha}{2(N_L)_{\alpha\alpha} + (N_L)_{\alpha\beta}}$$

where $(V_V)_\alpha$ is the volume fraction of the carbide phase, and $(N_L)_{\alpha\alpha}$ and $(N_L)_{\alpha\beta}$ are the average number of intercepts per unit length of test lines with the traces of the carbide/carbide grain boundary and carbide/binder interface, respectively.

- Contiguity of the carbide phase

$$C_\alpha = \frac{2(N_L)_{\alpha\alpha}}{2(N_L)_{\alpha\alpha} + (N_L)_{\alpha\beta}}$$

- Binder mean free path

$$\bar{L}_\beta = \bar{L}_\alpha \frac{(V_V)_\beta}{[1 - (V_V)_\beta][1 - (C_\alpha)]}$$

where $(V_V)_\beta$ is the volume fraction of the binder phase.

2.3.3 Magnetic Coercivity

To investigate the distribution of metal phase and the microstructural features outlined in section 2.3.2, the magnetic coercivity of the sintered specimens was measured.

2.3.4 Mechanical Properties

2.3.4.1 *Transverse Rupture Strength*

The transverse rupture strength (TRS) of as-sintered specimens was determined under three-point loading according to ASTM specification B406-76 (Ref 19). The maximum rupture load at the failure point of the test piece was used to calculate TRS:

$$\text{TRS (MPa)} = \frac{3PL}{2WT^2}$$

where P is breaking load (MN), L is length (m), W is width (m), and T is thickness (m). For each set of specimens, four tests were performed and the average value reported.

2.3.4.2 *Hardness*

Hardness of the sintered compacts was measured on a Vickers hardness testing machine (load, 30 kg) (Ref 20). About five indentations were taken on each polished specimen and the average value reported.

2.3.4.3 *Indentation Fracture Toughness*

Indentation fracture toughness (K_c) was measured according to the method suggested by Shetty et al. (Ref 21), based on Palmqvist crack geometry:

$$K_c(\text{MPa}\sqrt{\text{m}}) = 0.0319\ P/al^{1/2}$$

where P is indentation load (MN), a is half indentation diagonal (m), and l is Palmqvist crack length (m).

Testing was carried out at a load of 60 kg for grades containing cobalt and cobalt/nickel binders and at a load of 100 kg for grades containing nickel binder. A Vickers hardness testing machine was used to make the indentations. Crack length was measured using a precision measuring microscope (least count = 0.001 mm). Removal of subsurface damage or any surface layer that might have come under compression during postsintering cooling (Ref 21) was ensured by doubling the duration of each lapping/polishing stage discussed earlier. About five indentations were taken on each sample and the average value reported.

2.3.5 Corrosion Resistance

Measurements for evaluating corrosion resistance were carried out following ASTM specification G31-72 (Ref 22). The minimum exposure time was fixed per the ASTM-approved relation:

$$\text{Hours} = \frac{2000}{\text{Corrosion rate in mils per year (mpy)}}$$

The corrosion rate was calculated using the formula:

$$\text{Corrosion rate (mpy)} = 3.45 \times 10^6 \frac{W}{A \times T \times D}$$

where W is the mass loss in grams to the nearest 1 mg, A is the area of the specimen in square centimeters to the nearest 0.01 cm^2, T is the time of exposure in hours to the nearest 0.01 h, and D is the density of the specimen (g/cm^3).

3. Results and Discussion

3.1 *Sintered Porosity*

The densification behavior of the various cemented carbide grades tested is shown in Fig. 1. Nickel as a binder with WC appears to adversely affect densification. Small amounts of Cr_3C_2 when substituted in conjunction with nickel raises the porosity level. Nevertheless, comparatively greater Cr_3C_2 substitution levels again improve densification.

Both WC and Cr_3C_2 have poor wettability by nickel melted in a hydrogen atmosphere (Ref 23, 24). This accounts for the decrease in densification at lower levels of Cr_3C_2 in the alloys with nickel binder. Substitution of Cr_3C_2 for WC causes an in-

Table 1 Compositions of tested grades of cemented carbides

Hard phase, vol %		Binder, vol %		Hard phase, wt %		Binder, wt %	
WC	Cr_3C_2	Cobalt	Nickel	WC	Cr_3C_2	Cobalt	Nickel
83.5	0	16.5	...	90.00	...	10.00	...
81.5	2	16.5	...	88.95	0.93	10.12	...
79.5	4	16.5	...	87.85	1.90	10.25	...
77.5	6	16.5	...	86.73	2.87	10.40	...
71.5	12	16.5	...	83.23	5.97	10.80	...
83.5	0	8.25	8.25	90.00	...	5.00	5.00
81.5	2	8.25	8.25	88.92	0.93	5.06	5.09
79.5	4	8.25	8.25	87.83	1.90	5.12	5.15
77.5	6	8.25	8.25	86.73	2.87	5.18	5.22
71.5	12	8.25	8.25	83.22	5.97	5.39	5.42
83.5	0	...	16.5	90.00	...	...	10.00
81.5	2	...	16.5	88.90	0.93	...	10.17
79.5	4	...	16.5	87.80	1.90	...	10.30
77.5	6	...	16.5	86.70	2.87	...	10.43
71.5	12	...	16.5	83.20	5.97	...	10.83

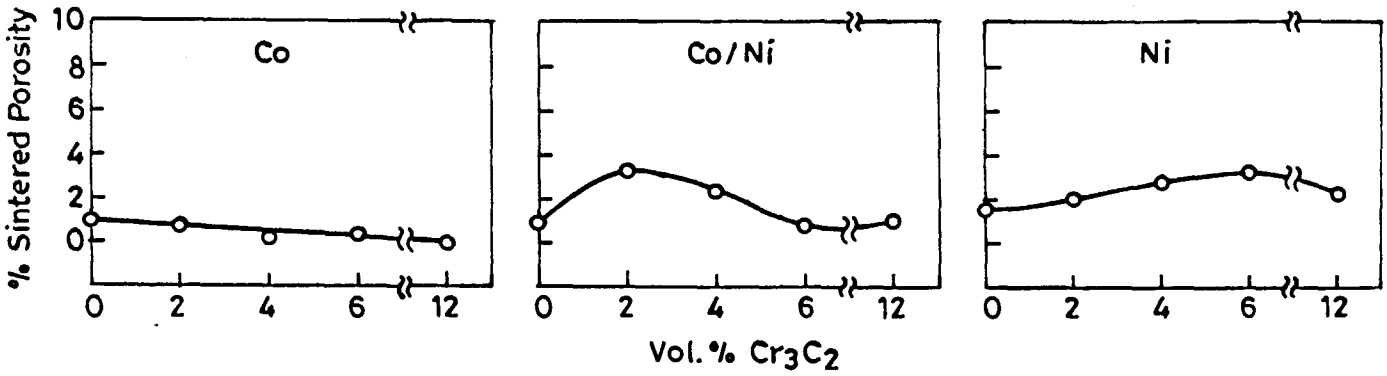

Fig. 1 Effect of Cr_3C_2 addition and binder-phase substitution on the sintered porosity of WC-10Co cemented carbide

creased carbon level in the system, as the former contains 13.33 wt% C—almost double the content in WC (6.13 wt%). Increased carbon content causes a greater amount of liquid to form during liquid-phase sintering (Ref 25), and the temperature at which liquid starts to form during sintering is lowered. This is due to the lowering of the solidus temperature within the two-phase range, which in the case of nickel binders may be as large as 70 to 80 °C (Fig. 2) (Ref 10). These two factors improve densification with higher levels of Cr_3C_2 substitution.

3.2 *Microstructure and Quantitative Metallography*

The microstructures of the cemented carbides (Fig. 3) consist of prismatic grains of WC embedded in the binder matrix. Ideally, a WC grain should be shaped like a truncated, flat, triangular prism. Any deviation from this shape, including round corners of the grains, is indicative of the existence of solution-reprecipitation and coalescence stages during sintering and a nonequilibrium condition while cooling down from the sintering temperature. The most discernible effect of Cr_3C_2 addition is refinement of the WC grains, evidenced by the microstructures as well as by quantitative metallographic study (Fig. 4, Table 2). The refining effect of Cr_3C_2 is more prominent in the compositions where nickel is substituted for cobalt. Any tendency toward discontinuous grain growth after nickel substitution is eliminated by Cr_3C_2 addition.

Quantitative metallographic study shows that Cr_3C_2 refines the WC grains regardless of binder type. Although in some compositions with high Cr_3C_2 substitution levels the average grain size increased, it is always smaller than that in the starting composition. Contiguity exhibited no regular trend. Binder mean free path increased after small additions of Cr_3C_2 in all three binder types, but after further additions exhibited no regularity in its variation.

3.3 *Magnetic Coercivity*

Substitution of a small amount of Cr_3C_2 (2 vol%) raises the magnetic coercivity value regardless of binder type; this is suggestive of hard-phase grain refinement (Fig. 5). In the cobalt-bonded alloys, 12 vol% Cr_3C_2 substitution causes the coercivity to rise appreciably, a phenomenon not observed in the alloys containing nickel. This rise may be due to the precipitation of a fine, nonmagnetic phase such as Co_3W within the binder. This proposition is supported by various work (Ref 26, 27).

3.4 *Mechanical Properties*

3.4.1 Transverse Rupture Strength

Addition of relatively little Cr_3C_2 (2 vol%) improves the TRS of WC-10Co cemented carbide, but this property drops almost linearly with increased Cr_3C_2 substitution (Fig. 6). This initial increase in TRS occurs because of grain refinement and an increase in binder mean free path (Fig. 4). The subsequent drop in TRS can be explained as follows.

The chief cause of strengthening in WC-Co alloys is the solid-solution strengthening of the binder cobalt by tungsten. Tungsten, having a greater atomic radius (1.37 Å) than cobalt (1.25 Å), puts the cobalt lattice under compression. Chromium, with an atomic radius identical to that of cobalt, cannot strengthen the cobalt lattice through a solid-solution mechanism. Chromium carbide is not soluble in WC (Ref 28); an x-ray diffraction study by Oakes (Ref 2) established that chromium stays entirely in the binder phase. Because cobalt does not have an unlimited solubility for carbides, the dissolution of Cr_3C_2 in the former should be accompanied by a rejection of WC from the binder. This is also evidenced by the fact that the free energy of formation for WC (39.9 KJ/mol at 1200 K) is lower than that for Cr_3C_2 (103.14 KJ/mol) (Ref 6). It can thus be concluded that the removal of dissolved tungsten from

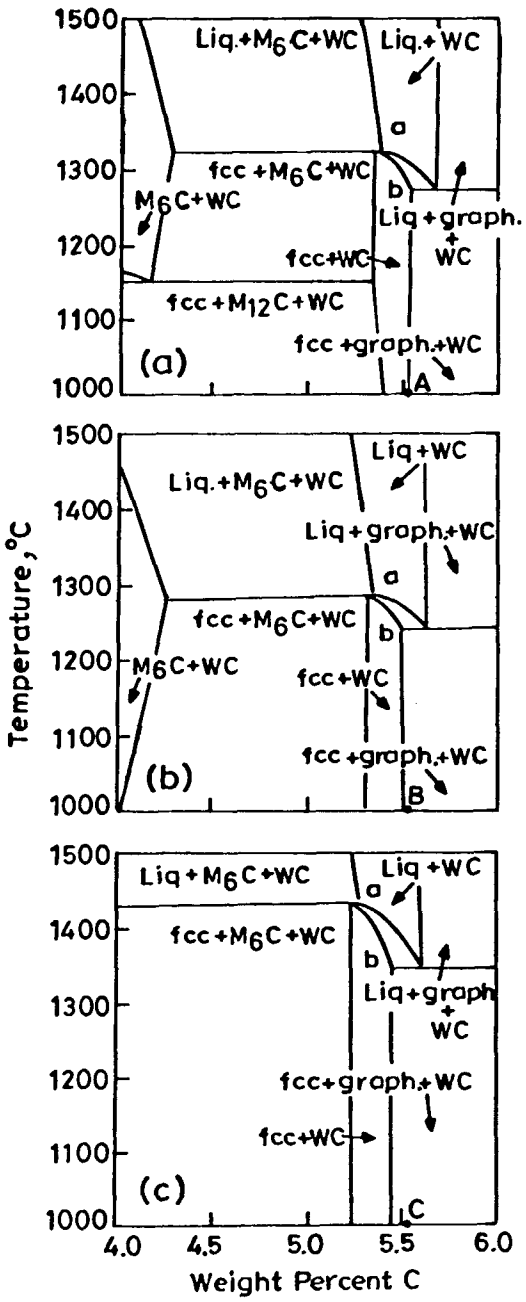

Fig. 2 Vertical sections of the Co-W-C (a), Co-Ni-W-C (Co:Ni = 4:1 by wt%) (b), and Ni-W-C (c) phase diagrams calculated at 10 wt% metallic binder

the binder phase as WC is the cause of loss in strength at higher levels of Cr_3C_2 substitution.

Substitution of nickel for cobalt results in higher porosity, thereby negating the beneficial effect of the initial Cr_3C_2 addition (Fig. 6). It is interesting to note that in the case of cemented carbides containing 12 vol% Cr_3C_2, the sintered porosity level is almost the same, but the TRS drops in the following order: nickel, cobalt/nickel, cobalt. This is because tungsten is more

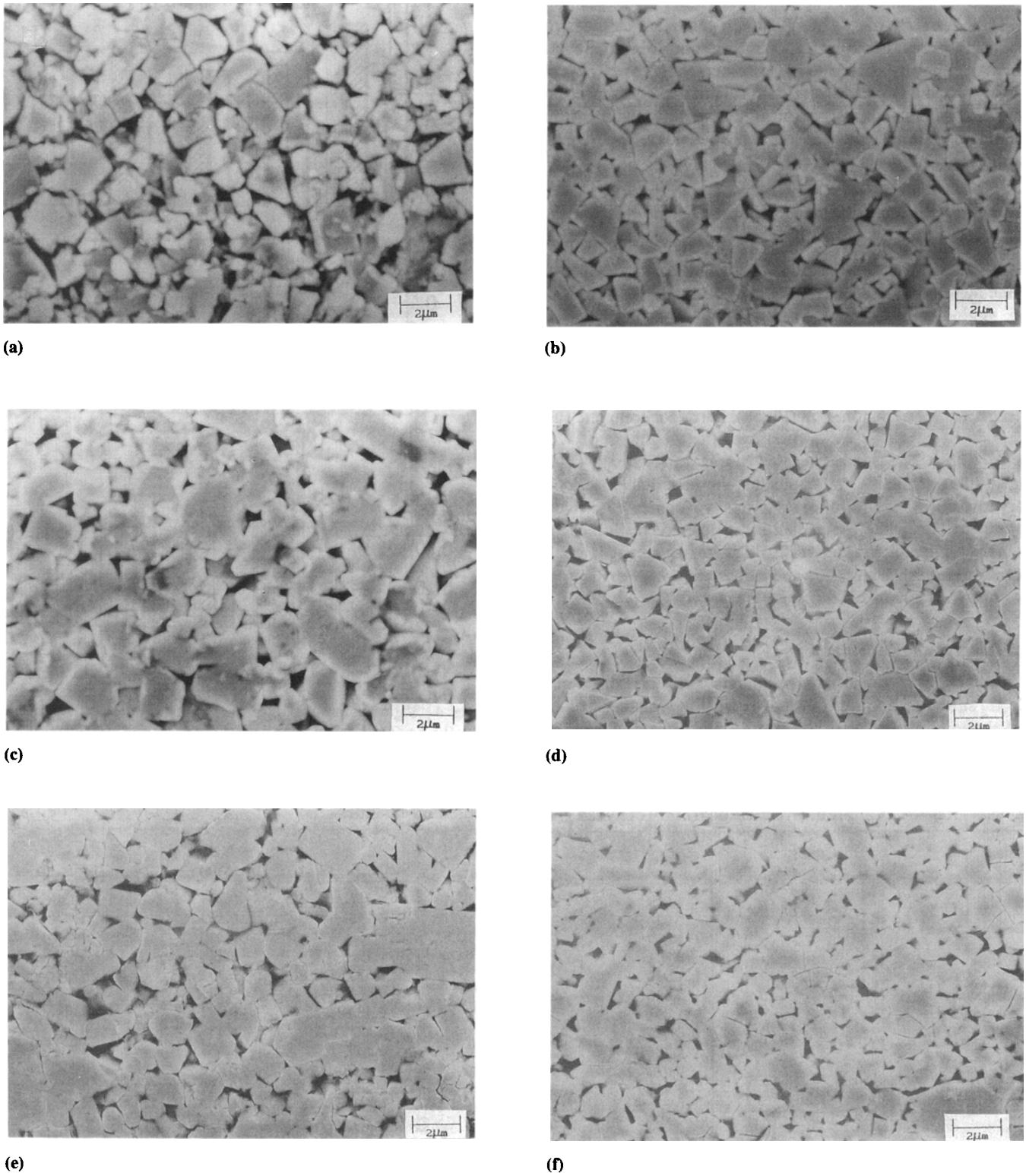

Fig. 3 SEM microstructures of some typical cemented carbides with or without Cr_3C_2 addition. (a) WC-10Co. (b) WC-2Cr_3C_2-10Co. (c) WC-10Co/Ni. (d) WC-2Cr_3C_2-10Co/Ni. (e) WC-10Ni. (f) WC-2Cr_3C_2-10Ni

soluble in nickel (14 to 30%) than in cobalt (4 to 19%) (Ref 10). Even after the removal of some dissolved tungsten from the binder following Cr_3C_2 addition, nickel would have a higher tungsten content and thus give better strengthening than cobalt.

3.4.2 Hardness

The Vickers hardness of WC-10Co cemented carbides remains almost unaltered by Cr_3C_2 substitution (Fig. 7). Substitution of cobalt by nickel, however, lowers the hardness, which can be attributed to the lower flow stress of nickel compared to cobalt. The inhomogeneity in the microstructure resulting from the incompatibility between Cr_3C_2 and nickel is reflected in the hardness variations in the nickel-bonded grades.

3.4.3 Indentation Fracture Toughness

The indentation fracture toughness value obtained for WC-10Co in the present study is slightly higher than those reported in the literature (Ref 17). This could be due to the loose, spherical, agglomerate morphology of the cobalt powder selected, which is different from the angular, chainlike morphology of cobalt powders conventionally used in the cemented carbide industry.

With Cr_3C_2 substitution, variation in toughness follows a pattern similar to that in TRS (Fig. 8). Partial or complete substitution of cobalt by nickel improves the toughness of WC-10Co alloy. The appearance of pores after small Cr_3C_2 substitutions in these grains negates the beneficial effect observed in cobalt-bonded alloys. Hardness of cemented carbides is known to bear an inverse relationship to crack resistance and thus to fracture toughness (Ref 29). The improvement of toughness after nickel substitution and its variation with Cr_3C_2 additions can be explained along these lines.

3.5 *Corrosion Resistance*

Results of corrosion experiments (Fig. 9) show that Cr_3C_2 substitution improves the corrosion resistance of cobalt-bonded alloys. Substitution of nickel for cobalt with concurrent Cr_3C_2 substitution produces even better corrosionresistance. The present study, in contrast to the findings of Kny and Schmid (Ref 30), shows that 6 N HNO_3 is a stronger corroding medium than 2N H_2SO_4.

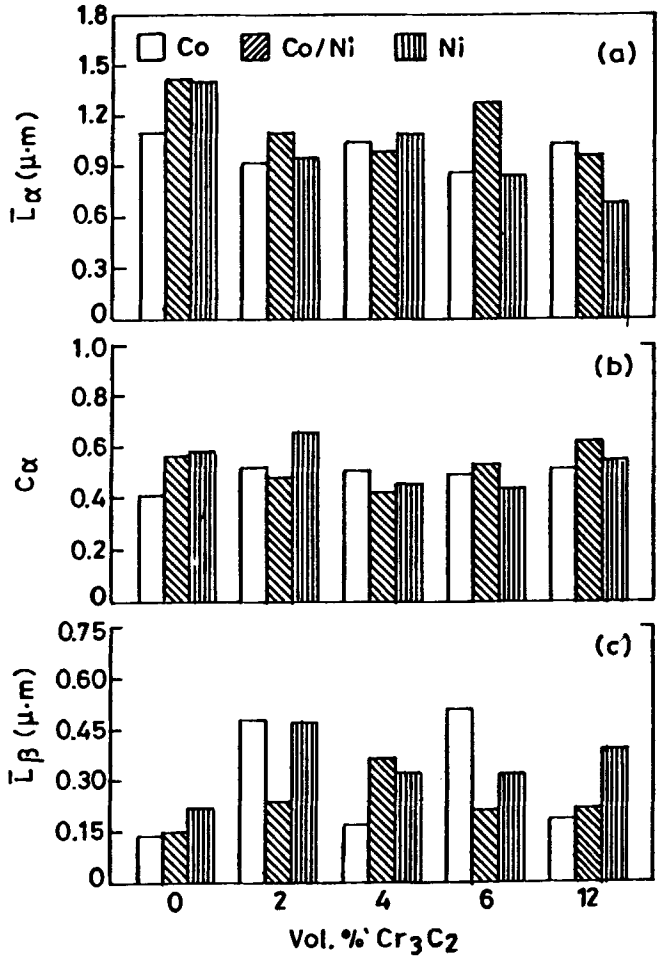

Fig. 4 Variation of mean linear intercept grain size (a), contiguity (b), and binder mean free path (c) in hard- and binder-phase-modified WC-10Co cemented carbides

Table 2 Results of quantitative metallography of tested grades of cemented carbides

Binder type	Cr_3C_2 content, vol %	$\bar{L}_\alpha$, μm	S.D. (σ)(a)	C_α	S.D. (σ)(a)	$\bar{L}_\beta$, μm
Cobalt	0	1.099	0.149	0.412	0.187	0.138
	2	0.920	0.158	0.158	0.163	0.480
	4	1.049	0.131	0.508	0.140	0.171
	6	0.871	0.074	0.496	0.188	0.516
	12	1.040	0.195	0.523	0.151	0.190
Cobalt/nickel	0	1.416	0.161	0.566	0.171	0.149
	2	1.091	0.120	0.480	0.083	0.238
	4	0.975	0.119	0.423	0.138	0.368
	6	1.286	0.206	0.538	0.194	0.218
	12	0.973	0.146	0.636	0.216	0.222
Nickel	0	1.400	0.246	0.582	0.189	0.220
	2	0.950	0.099	0.660	0.120	0.466
	4	1.096	0.171	0.460	0.138	0.327
	6	0.860	0.087	0.440	0.108	0.322
	12	1.000	0.073	0.558	0.130	0.400

(a) S.D. (σ) = population standard deviation = $[(\Sigma x^2 - n\bar{x}^2)/n]^{1/2}$

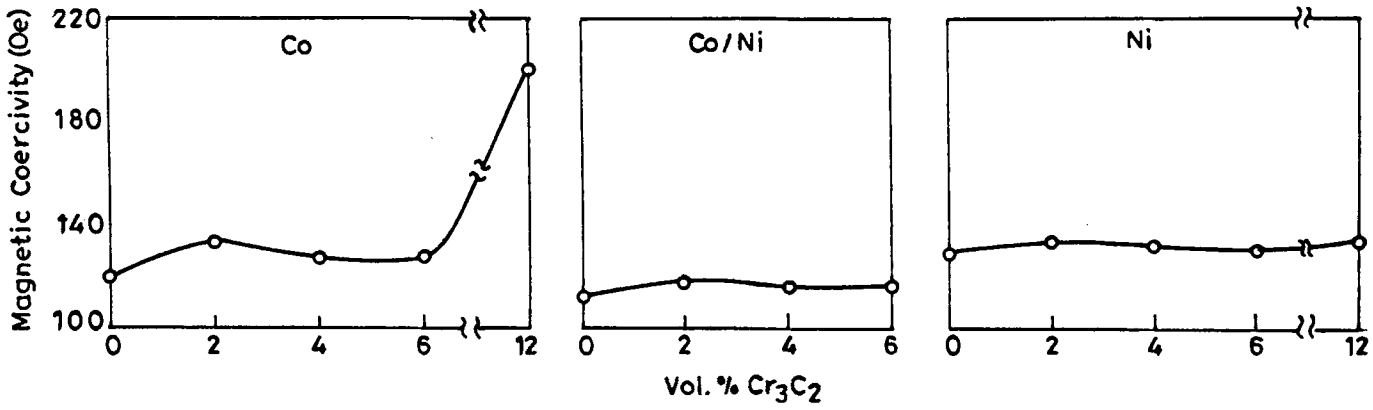

Fig. 5 Variation of the magnetic coercivity of WC-10Co cemented carbide with Cr_3C_2 substitution and binder modification

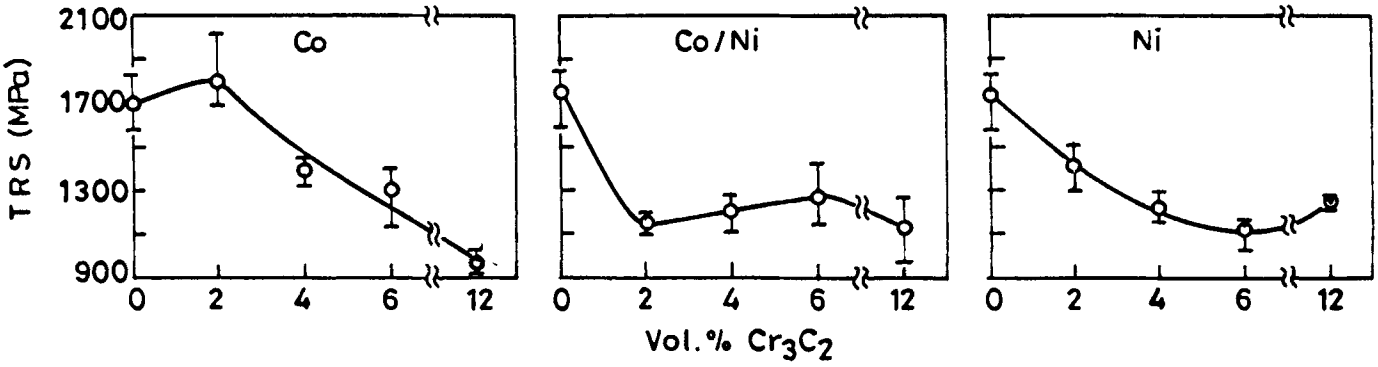

Fig. 6 Effect of hard-phase and binder-phase modifications on the TRS of WC-10Co cemented carbide

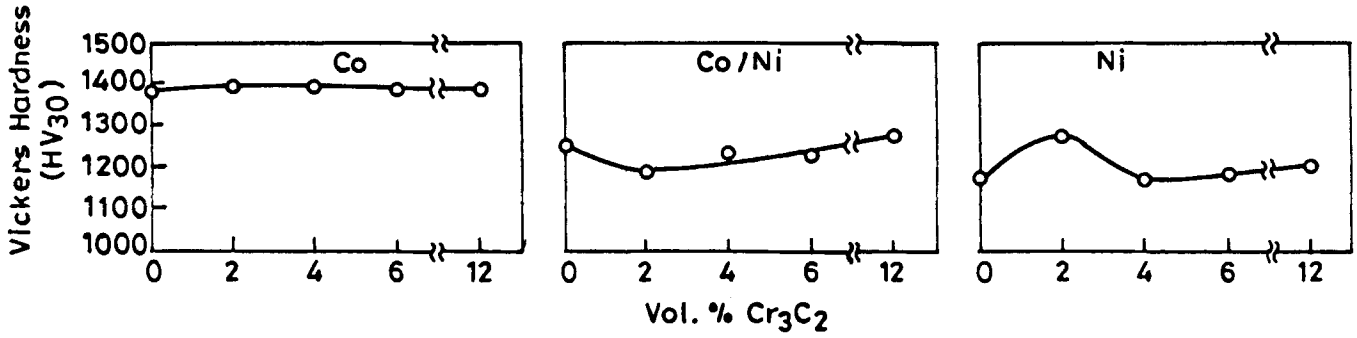

Fig. 7 Effect of hard-phase and binder-phase modifications on the Vickers hardness of WC-10Co cemented carbide

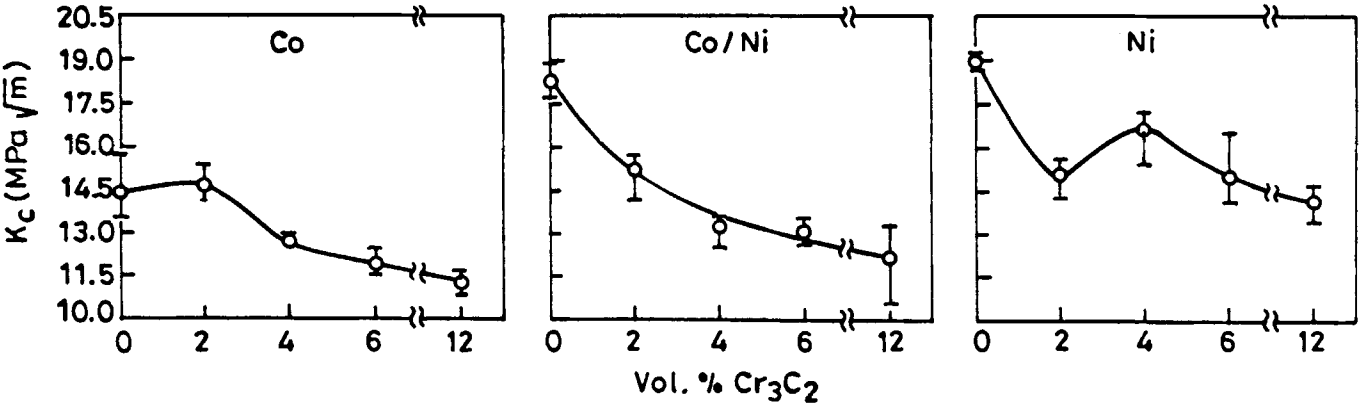

Fig. 8 Effect of hard-phase and binder-phase modifications on the indentation fracture toughness of WC-10Co cemented carbide

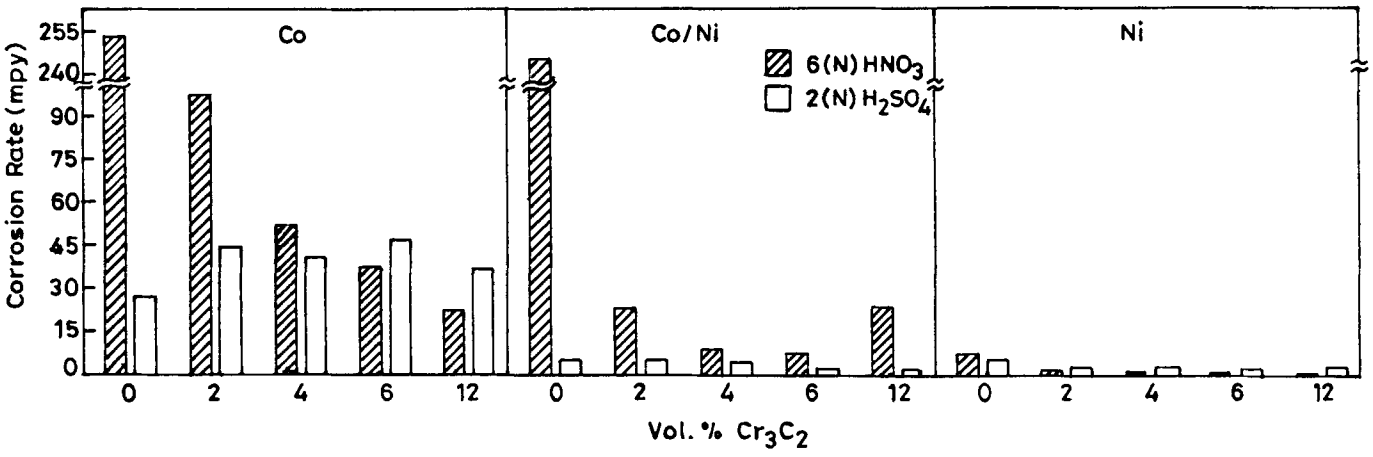

Fig. 9 Variation of corrosion rates of different hard- and binder-phase-modified cemented carbides in 6 *N* HNO_3 and 2 *N* H_2SO_4 solutions, respectively

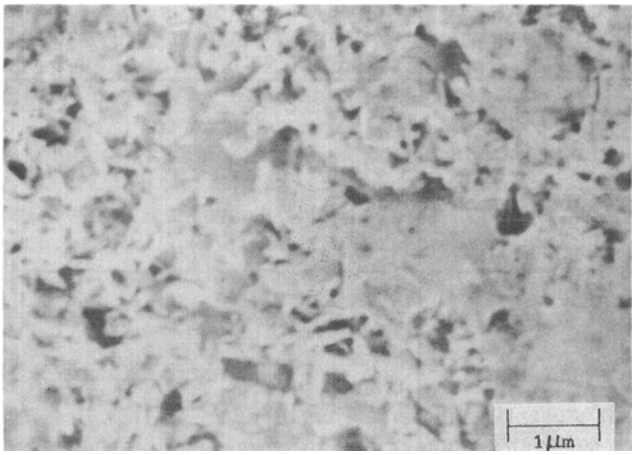

(a)

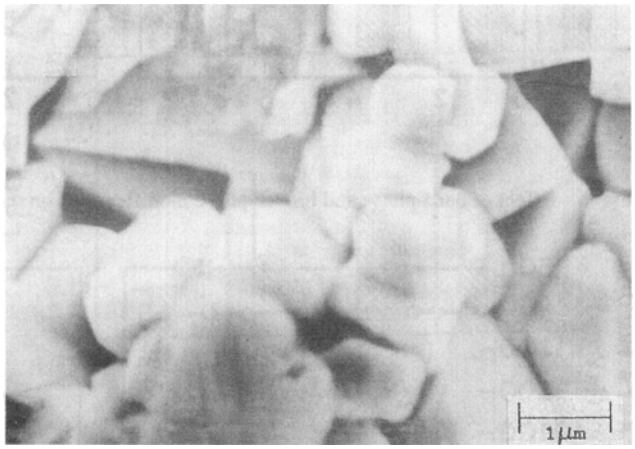

(b)

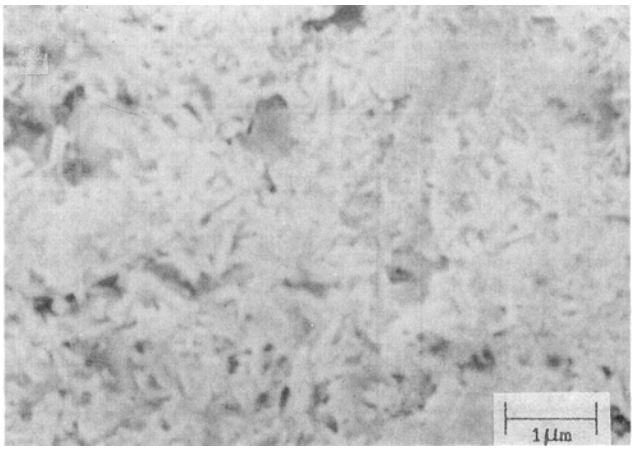

(c)

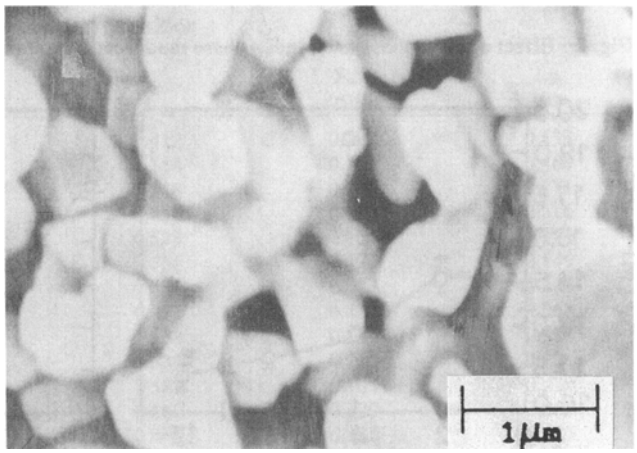

(d)

Fig. 10 Typical SEM microstructures of corroded cemented carbide specimens. (a) WC-10Co (HNO_3). (b) WC-10Co (H_2SO_4). (c) WC-12Cr_3C_2-10Ni (HNO_3). (d) WC-12Cr_3C_2-10Ni (H_2SO_4)

Scanning electron micrographs (Fig. 10) of the corroded samples reveal that attack by sulfuric acid is more prominent in the binder phase, whereas nitric acid attacks both hard phases and binder phases. The presence of chromium in nickel binder and the passivation response of these metals accounts for the higher corrosion resistance of the modified grades of cemented carbides.

4. Conclusions

Based on the foregoing results and discussion, a number of conclusions can be drawn:

- Chromium carbide does not affect the densification of WC-10Co cemented carbides. Substitution of cobalt by nickel, at least with low Cr_3C_2 additions, is not favorable for densification.
- Chromium carbide refines the carbide grains in WC-base cemented carbides, regardless of binder type, thus eliminating any tendency toward discontinuous grain growth.
- Magnetic coercivity variation suggests a grain refinement in the hard phase upon Cr_3C_2 addition. Precipitation of a fine, nonmagnetic phase in the binder in the case of cobalt-bonded alloy upon a large volume fraction of Cr_3C_2 substitution is also possible.
- Addition of up to 2 vol% Cr_3C_2 in WC-10Co cemented carbides increases TRS and K_c values. However, large amounts of such additions have the reverse effect. Cobalt binder modification lowers TRS values but substantially improves K_c values.
- The Vickers hardness of WC-10Co cemented carbide is not much altered by Cr_3C_2 addition. Binder modification has a negative effect on hardness.
- The addition of Cr_3C_2 greatly improves the corrosion resistance of WC-10Co hard metals. For any cobalt-bonded cemented carbide, the partial or complete substitution of cobalt by nickel enhances corrosion resistance.

References

1. C.T. Peters and S.M. Brabyn, Properties of Nickel Substituted Hardmetals and Their Performance in Hard Rock Drill Bits, *Met. Powder Rep.*, Vol 42 (No. 12), 1987, p 863-865
2. J.J. Oakes, Effect of Cr and Mo Additions to the Binder Phase of Cemented Carbides Used for Rod Mill Rolls, *Met. Powder Rep.*, Vol 42 (No. 7/8), 1987, p 492-499
3. E.A. Almond and B. Roebuck, Some Characteristics of Very Fine Grained Hard Metals, *Met. Powder Rep.*, Vol 42 (No. 7/8), 1987, p 512-515
4. A. Egami, T. Kusaka, M. Machida, and K. Kobayashi, Ultra Submicron Hardmetals for Miniature Drills, *Met. Powder Rep.*, Vol 44 (No. 12), 1989, p 822-826
5. S. Inada and H. Yoshimura, Material Properties and End Milling Performance of WC-10%Co-0.75%-Cr_3C_2 Micrograin Cemented Carbide, *Proc. 13th Plansee Seminar*, Vol 2, H. Bildstein and R. Eck, Ed., Metallwerk Plansee, Reutte, Austria, 1993, p 67-79
6. L. Yao and C. Yang, Effect of Refractory Carbide Additions on the Characteristics of Binder Phase in WC-Co Hard Alloys, *Advances in Powder Metallurgy and Particulate Materials*, Vol 8, J.M. Capus and R.M. German, Ed., Metal Powder Industries Federation, 1992, p 61-63
7. V. Campagnulo, Modern Techniques of Hard Metal Production, *Met. Powder Rep.*, Vol 48 (No. 4), 1993, p 36-40
8. L.J. Prakash, Properties of Submicron WC-Based Cemented Carbides, *Met. Powder Rep.*, Vol 44 (No. 12), 1989, p 835-838
9. E.A. Almond and B. Roebuck, Very Fine Grained Hardmetals, *Int. J. Refract. Hard Met.*, Vol 6 (No. 3), 1987, p 137-144
10. L. Prakash, A Review of the Properties of Tungsten Carbide Hardmetals with Alternative Binder Systems, *Proc. 13th Int. Plansee Seminar*, Vol 2, H. Bildstein and R. Eck, Ed., Metallwerk. Plansee Reutte, Austria, 1993, p 80-109
11. S. Ekemer, L. Lindholm, and T. Hartzell, Aspects on Nickel as a Binder Metal in WC-Based Cemented Carbides, *Proc. 10th Plansee Seminar*, Vol 1, H.M. Ortner, Ed., Metallwerk Plansee, Reutte, Austria, 1981, p 477-492
12. K.Y. Eun, D.Y. Kim, and D.N. Yoon, Variation of Mechanical Properties with Ni/Co Ratio in WC-(Co-Ni) Hardmetals, *Powder Metall.*, Vol 27 (No. 2), 1984, p 112-114
13. J.M. Barranco and RA. Warenchak, Liquid Phase Sintering of Carbides Using Nickel-Molybdenum Alloy, *Int. J. Refract. Met. Hard Mater.*, Vol 8 (No. 2), 1989, p 102-110
14. B. Roebuck and E.A. Almond, A Comparison of the Deformation Characteristics of Co and Ni Alloys Containing Small Amounts of W and C, *Proc. 10th Plansee Seminar*, Vol 1, H.M. Ortner, Ed., Metallwerk Plansee, Reutte, Austria, 1981, p 493-508
15. S.M. Brabyn, R. Cooper, and C.T. Peters, Effects of the Substitution of Nickel for Cobalt in WC Based Hardmetal, *Proc. 10th Plansee Seminar, Vol 2, H.M. Ortner, Ed., Metallwerk. Plansee, Reutte, Austria, 1981, p 675-692*
16. R. Roebuck, E.A. Almond, and A.M. Cottenden, The Influence of Composition, Phase Transformation and Varying the Relative FCC and HCP Phase Contents on the Properties of Dilute Co-W-C Alloys, *Mater. Sci. Eng.*, Vol 66 (No. 2), 1984, p 179-194
17. S.K. Bhaumik, G.S. Upadhyaya, and M.L. Vaidya, Alloy Design of WC-10Co Hard Metals with Modification in Carbide and Binder Phase, *Int. J. Refract. Met. Hard Mater.*, Vol 11 (No. 1), 1992, p 9-22
18. J. Gurland, Application of Quantitative Microscopy to Cemented Carbides, *Practical Application of Quantitative Metallography*, STP 839, J.L. McCall and J.H. Steele, Jr., Ed., ASTM, 1984, p 65-84
19. "Standard Test Method for Transverse Rupture Strength of Cemented Carbides," B406-76, *Annual Book of ASTM Standards*, Vol 02.05, Section 2, ASTM, 1987, p 208-209
20. C.B. Ponton and R.D. Rawlings, Vickers Indentation Fracture Toughness Test, Part I: Review of Literature and Formulation of Standardized Indentation Toughness Equations, *Mater. Sci. Technol.*, Vol 5 (No. 9), 1989, p 870
21. D.K. Shetty, I.G. Wright, P.N. Mincer, and A.H. Clauer, Indentation Fracture of WC-Co Cermets, *J. Mater. Sci.*, Vol 20 (No. 5), 1985, p 1873-1882
22. "Standard Practice for Laboratory Immersion Corrosion Testing of Metals," G31-72, *Annual Book of ASTM Standards*, Vol 03.02, Section 3, ASTM, 1987, p 176-186
23. G.V. Samsonov, V.K. Vitryanuk, and F.I. Chapligin, *Tungsten Carbides*, Naukova Dumka, Kiev, 1974, p 60 (in Russian)
24. V.A. Tracey, Nickel in Hard Metals, *Int. J. Refract. Met. Hard Mater.*, Vol 11 (No. 3), 1992, p 142
25. B. Uhrenius, Evaluation of Molar Volumes in the Co-W-C System and Calculation of Volume Fractions of Phases in Cemented Carbides, *Proc. 13th Int. Plansee Seminar*, Vol 2, H. Bildstein and R. Eck, Ed., Metallwerk Plansee, Reutte, Austria, 1993, p 188-199

26. J. Freytag and H.E. Exner, The Influence of Tungsten and Carbon Additions on the Sintering and Magnetic Properties of WC-12Co Cemented Carbide, *Modern Developments in Powder Metallurgy,* Vol 10, H.H. Hausner and P.V. Taubenblat, Ed., Metal Powder Industries Federation, 1977, p 511-523

27. D.I. Tillwick and I. Joffe, Magnetic Properties of Co-W Alloys in Relation to Sintered WC-Co Compacts, *Scr. Metall.,* Vol 7 (No. 5), 1973, p 479-484

28. P. Stecher, F. Benesovsky, and H. Nowotny, *Planseeber. Pulvermet,* Vol 12, 1964, p 89

29. R. Warren and H. Matzke, Indentation Testing of a Broad Range of Cemented Carbides, *Science of Hard Materials,* R.K. Viswanadham, D.J. Rowcliffe, and J. Gurland, Ed., Plenum Press, 1983, p 563-582

30. E. Kny and L. Schmid, New Hardmetal Alloys with Improved Erosion and Corrosion Resistance, *Int. J. Refract. Mater. Met. Hard,* Vol 6 (No. 3), 1987, p145-148